A dynamic anode boosting sulfamerazine mineralization via electrochemical oxidation

Fengxia Deng[a], Jinyu Xie[a], Orlando Garcia-Rodriguez[d], Baojian Jing[a], Yingshi Zhu[a], Zhonglin Chen[a], Jyh-Ping Hsu[c], Jizhou Jiang[b,*], Shunwen Bai[a,*], Shan Qiu[a,*]

[a] State Key Laboratory of Urban Water Resources Centre, School of Environment, Harbin Institute of Technology, Harbin, 150090, P. R. China

[b] School of Environmental Ecology and Biological Engineering, School of Chemistry and Environmental Engineering, Key Laboratory of Green Chemic al Engineering Process of Ministry of Education, Wuhan Institute of Technology, Wuhan, Hubei, 430205, P. R. China.

[c] Department of Chemical Engineering, National Taiwan University, Taipei 10617, Taiwan

[d] Centre for Water Research, Department of Civil and Environmental Engineering, National University of Singapore, 1 Engineering Dr. 2, Singapore, 117576, Singapore

*Corresponding author:

027wi@163.com (Jizhou Jiang), Shunwen Bai (baishunwen@hit.edu.cn), qiushan@hit.edu.cn (Shan Qiu)

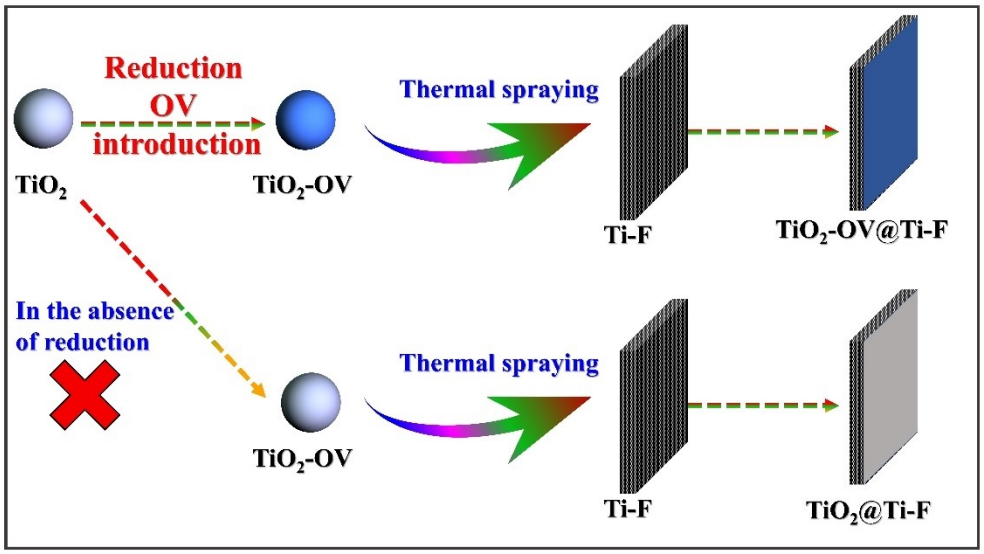

Fig. S1. The process to fabricate anodes in the absence and presence of oxygen vacancies.

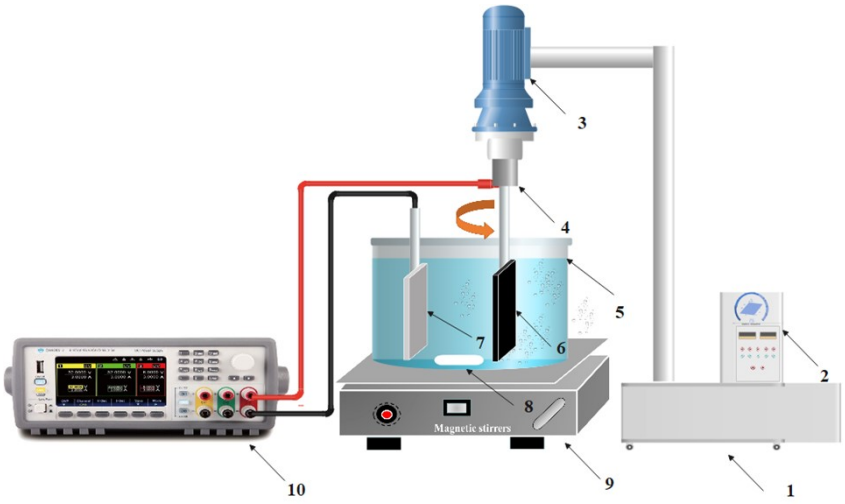

Fig. S2. The designed rotating system of electrochemical setup for SMR degradation. (1) trestle table, (2) rotational speed control system, (3) electrical machinery, (4) dynamo brush, (5) undivided single cell, (6) the designed anode, (7) count cathode, (8) magnet rotor, (9) magnetic stirrer; (10) DC power.

SI.1 DFT calculation

Calculations on electronic ground state, cationic and anionic geometries described in this paper were performed at the DFT levels of theory as implemented within the Gaussian 03 software package [1] on the SGI origin 2000 server. Becke's three-parameter hybrid method using the Lee-Yang-Parr correlation functional (B3LYP) was employed, which was proven to be a very useful in predicting geometries.

The geometry, electron density and population analysis of Ti_4O_7, H_2O, Ti_4O_7+H_2O, Ti_4O_7+HO·--·H, TiO_2, TiO_2+H_2O, TiO_2+HO·--·H were conducted using the plane-wave ultra-soft (PWUS) pseudo-potential method with the generalized gradient approximation (GGA) and correlation in the Perdew-Wang 91 (PW91) as implemented in the DMol3 DFT module of Materials Studio package calculation [2]. A hybrid semiempirical solution (OBS) was taken to introduce damped atom pairwise dispersion corrections of the form C_6R^{-6} in the DFT-D formalism. In module of geometry optimization, the quality of convergence tolerance is set as medium, and the energy is set as 2×10^{-5} Ha. The convergence criterion for the maximal force on atoms is 0.004 Ha/Å. The maximum displacement is 5×10^{-3} Å. The maximum iteration is set as 200 and the maximum step size is 0.3 Å. The cell is also optimized with optimization cycles of 2 and displacement step of 0.015 Å. In module of geometry optimization, the quality of convergence tolerance is set as medium, and the energy as 2×10^{-5} Ha. The convergence criterion for the maximal force on atoms is 0.004 Ha/Å. The maximum displacement is 5×10^{-3} Å. The maximum iteration is set at 200, and the maximum step size is 0.3 Å. The cell is also optimized with optimization cycles of 2 and displacement step of 0.015 Å. In module of electronic optimization, the integration accuracy and self-consistent field (SCF) tolerance are both set as medium. All electrons are core treatment with a double numeric plus polarization (DNP) basis

set and the orbital cutoff quality is set as medium. The SCF convergence accuracy is set at 1×10^{-4} eV/atom, and the maximum SCF cycles at 512. Multipolar expansion of Hexadecapole and a Smearing of 0.05 are adopted. These calculations were carried out on an Intel Pentium PC computer with 12 cores and 32 GB of memory. The space group of Ti_4O_7 crystal is $P\bar{1}$[2], and the crystal system is tetragonal. The lattice parameters of Ti_4O_7 are a=5.638 Å, b=6.957 Å, c=7.184 Å, α=64.178°, β=71.103°, and γ=75.110°. The space group of anatase TiO_2 crystal is $I4_1/amd$ [141], and the crystal system is tetragonal. The lattice parameters of TiO_2 are a=b=c=5.566 Å, α=β=140.054°, and γ=57.771°. The anatase (101) surface was modeled as a slab with four TiO_2 layers [3].

SI.2 Life cycle assessment

For TiO_2-OV@Ti-F anode, the primary data in life cycle inventory (LCI) were obtained via calculating the energy, chemical usage and environmental emissions along with whole laboratory experimental processes. Regarding other anodes, LCI was developed based on the existing information in the literature [4-6]. The secondary data utilized in background processes such as the production of electricity and chemicals, were taken from the ecoinvent 3.4 database. Details were given in **Table S1**.

Environmental impacts were assessed by the ReCiPe method comprising three environmental categories (ecosystem quality, human health, and resources) including a total of 17 end-point impact categories. To facilitate direct comparison between all the alternatives, a total environmental impact obtained by aggregating all the impact categories is used for each assessed anode. The relative impacts of each impact category were deduced by quantifying proportional correlation and conducting a contribution analysis to identify the major environmental contributors for each

alternative. To assess the robustness of the comparison outcome, a Monte Carlo simulation was performed to examine the uncertainty incurred by inventory variability. The use of open LCA software grants for the uncertainty propagation over inventory data with assumed normal distribution under 10000 independent simulations. In practice, the Monte Carlo simulation can be implemented throughout all the impact categories as well as the total environmental impacts. Since we mainly focused on the comparison of total environmental impact, the results of uncertainty test for other impact categories are presented in the Supporting Information (**Table S2-S4**).

A standardized four-step framework defined by the ISO 14040–14044 standards was used for LCA (International Organization for Standardization (ISO), 1997): i) goal and scope definition, ii) life cycle inventory, iii) life cycle impact assessment and IV) interpretation.

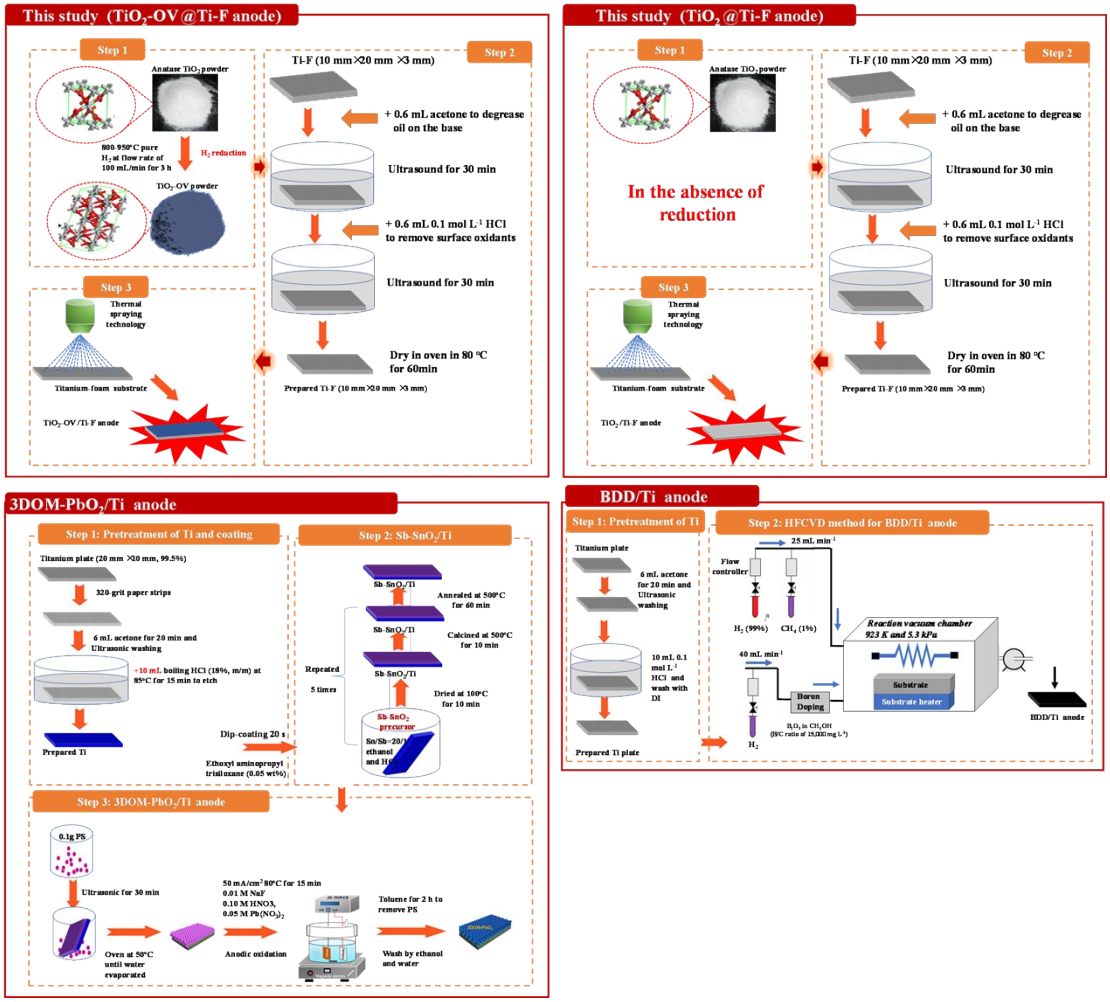

100

101 Fig. S3. Schematic representation of the production processes of the three anodic

102 materials used for LCA

Table S1. Life cycle inventory of the three anodic materials based on one functional unit (1 cm×2 cm anodic plate) and the system boundaries defined in this text

The anode	The chemicals and electricity during fabrication	The diagrams of the production processes
1. TiO_2-OV@Ti-F (this study)	**Step 1**: Pure H_2（99.99%）3.48×10^{-3} mL The required electricity during reduction=（0.98-1.16）× 10^{-6} kwh	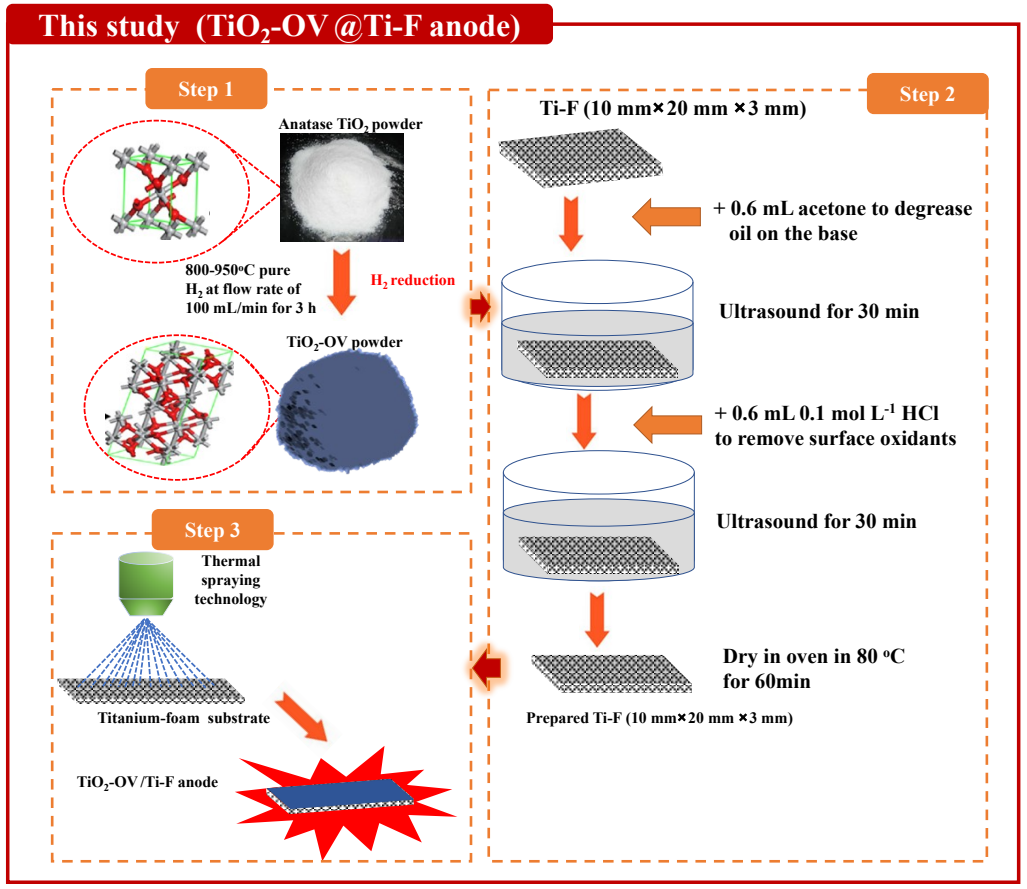
	Step 2: Ti-foam (1cm×2 cm) 1.3254 g Acetone 6 mL HCl 21.9 mg Ultrapure water100 mL The required electricity for ultrasound =2.9×10^{-4} kwh	
	Step 3: Pure Ar（99.99%）3.51×10^{-2} mL Pure H_2（99.99%）1.28×10^{-2} mL The required electricity =2.54×10^{-4} kwh	

2. TiO_2@Ti-F (this study)	**Step 1**: in the absence of H_2 reduction Pure H_2（99.99%）3.48×10^{-3} mL The required electricity during reduction=（0.98-1.16）× 10^{-6} kwh	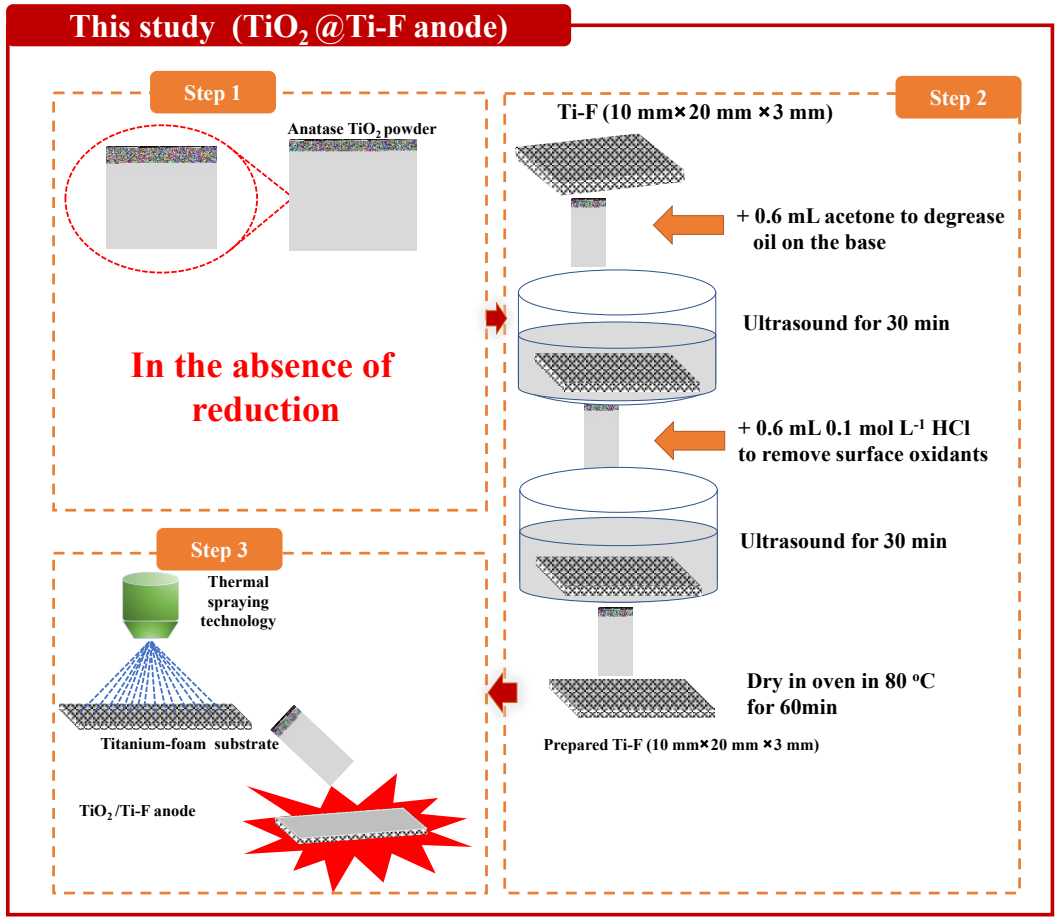
	Step 2: Ti-foam (1cm×2 cm) 1.3254 g Acetone 6 mL HCl 21.9 mg Ultrapure water100 mL The required electricity for ultrasound =2.9×10^{-4} kwh	
	Step 3: Pure Ar（99.99%）3.51×10^{-2} mL Pure H_2（99.99%）1.28×10^{-2} mL The required electricity =2.54×10^{-4} kwh	
	Step. 1 Ti pretreated Ti base （1cm×2 cm）：1.3254 g	

3. 3DM-PbO_2/Ti [6]	Acetone：6 mL 320 mesh sandpaper strip HCl: 180 mg Ultrapure water：100 mL The electricity =5.8×10^{-4} kwh	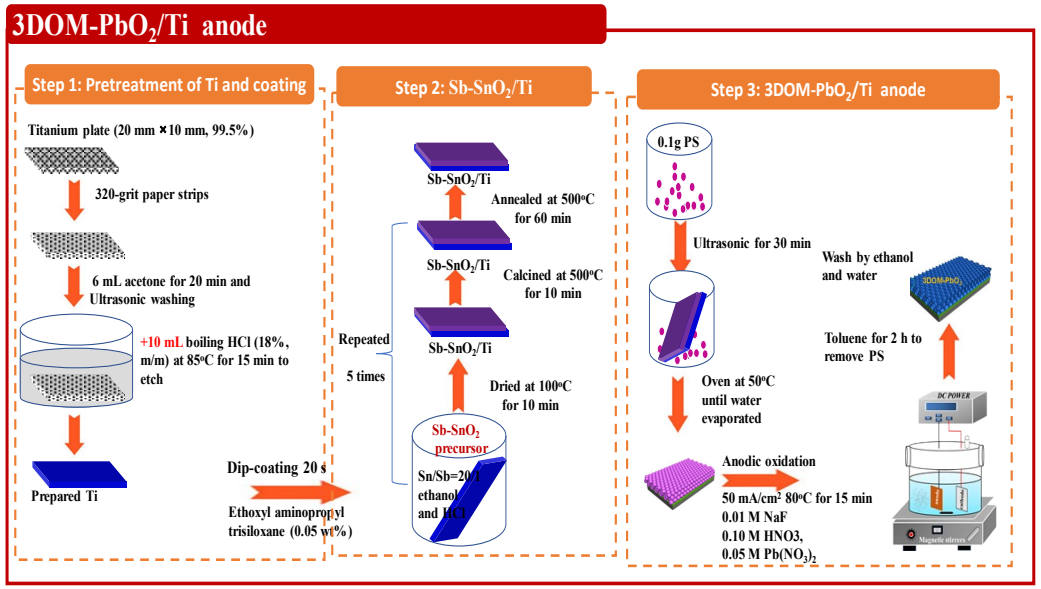
	Step. 2 dip-coating （Chemicals） ethoxyl aminopropyl trisiloxane 0.05 g $SnCl_4\times5H_2O$ 10g $SbCl_3$ 0.1g Ethanol 100 mL Concentrated HCl 1 mL Pure O_2=0.095 mL The energy used to heat using tube furnace=6.38×10^{-6} kwh	
	Step. 3 Polystyrene sphere 0.1 g 0.042g NaF, 0.63 g HNO3 1.66 g $Pb(NO_3)_2$, 100 g ultrapure water Ethanol 10 mL The electricity during anodic oxidation：8×10^{-4} kwh (current 0.4A，potential 20 V) The required electricity during anodic oxidation The electricity used to remove PS =1.2×10^{-6} kwh	
4. BDD/Ti Anode	**hot filament chemical vapor deposition (HFCVD) technique**	

[4]	**Step. 1** Acetone 6 mL HCl 0.8 mL The required electricity=5.0×10^{-4} kwh **Step 2:** H_2 225.7 mL CH_4 87.2 mL B_2O_3 4800 mg CH_3OH 320 mL The required electricity =43.608 kwh	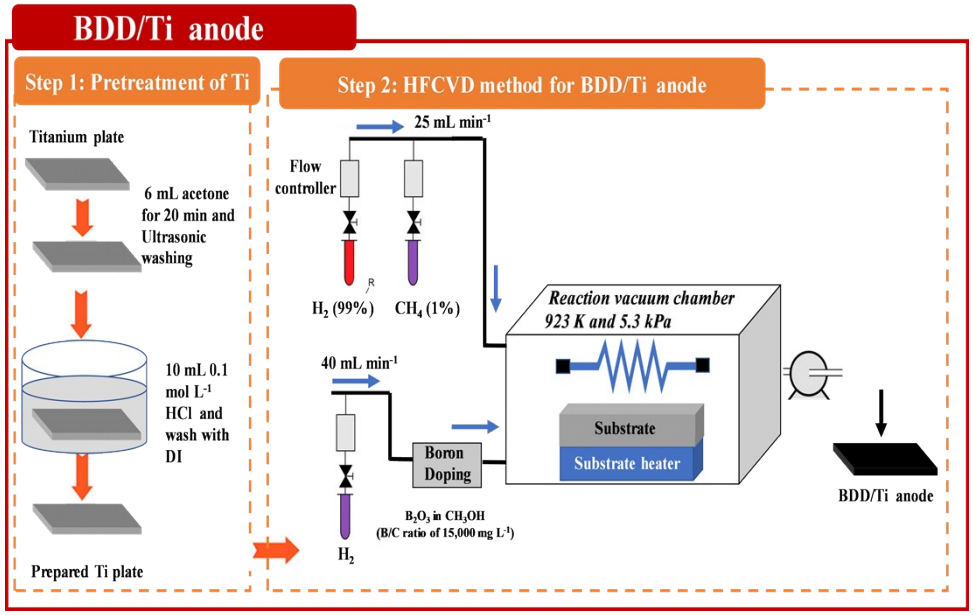

106

107

108

109

110

111

112

113

114

115

116

Table S2. Results of Monte Carlo simulation for assessing the environmental impact of TiO_2-OV@Ti-F

Impact categories	Units	Mean TEI	Standard deviation	Minimum TEI	Maximum TEI	Median TEI	5% Percentile	95% Percentile
ecosystem quality - agricultural land occupation	points	1.72E-06	1.68E-07	1.18E-06	2.27E-06	1.73E-06	1.43E-06	1.97E-06
ecosystem quality - climate change, ecosystems	points	1.32E-03	1.09E-04	9.70E-04	1.67E-03	1.32E-03	1.13E-03	1.49E-03
ecosystem quality - freshwater ecotoxicity	points	6.01E-07	5.21E-08	4.37E-07	7.71E-07	6.04E-07	5.07E-07	6.80E-07
ecosystem quality - freshwater eutrophication	points	1.45E-06	1.37E-07	1.02E-06	1.90E-06	1.46E-06	1.21E-06	1.66E-06
ecosystem quality - marine ecotoxicity	points	1.71E-04	1.63E-05	1.20E-04	2.25E-04	1.72E-04	1.42E-04	1.96E-04
ecosystem quality - natural land transformation	points	4.12E-04	3.89E-05	2.89E-04	5.39E-04	4.13E-04	3.43E-04	4.70E-04
ecosystem quality - terrestrial acidification	points	4.97E-06	4.13E-07	3.65E-06	6.31E-06	4.99E-06	4.25E-06	5.61E-06
ecosystem quality - terrestrial ecotoxicity	points	4.19E-06	3.63E-07	3.05E-06	5.38E-06	4.21E-06	3.54E-06	4.74E-06
ecosystem quality - total	points	1.93E-03	1.66E-04	1.40E-03	2.47E-03	1.94E-03	1.63E-03	2.18E-03
ecosystem quality - urban land occupation	points	1.37E-05	1.31E-06	9.53E-06	1.80E-05	1.37E-05	1.14E-05	1.57E-05
human health - climate change, human health	points	1.66E-03	1.38E-04	1.22E-03	2.10E-03	1.67E-03	1.42E-03	1.87E-03
human health - human toxicity	points	4.86E-03	4.64E-04	3.39E-03	6.37E-03	4.87E-03	4.03E-03	5.55E-03
human health - ionising radiation	points	7.79E-07	7.56E-08	5.38E-07	1.03E-06	7.80E-07	6.45E-07	8.90E-07
human health - ozone depletion	points	1.24E-07	1.19E-08	8.58E-08	1.62E-07	1.24E-07	1.03E-07	1.41E-07
human health - particulate matter formation	points	2.94E-04	2.61E-05	2.13E-04	3.79E-04	2.95E-04	2.48E-04	3.34E-04
human health - photochemical oxidant formation	points	2.37E-05	1.67E-06	1.80E-05	2.87E-05	2.37E-05	2.09E-05	2.64E-05
human health - total	points	6.83E-03	6.27E-04	4.87E-03	8.89E-03	6.85E-03	5.73E-03	7.77E-03
resources - fossil depletion	points	2.20E-03	1.58E-04	1.69E-03	2.68E-03	2.21E-03	1.94E-03	2.45E-03
resources - metal depletion	points	1.23E-04	1.19E-05	8.56E-05	1.62E-04	1.24E-04	1.02E-04	1.41E-04
resources - total	points	2.33E-03	1.68E-04	1.78E-03	2.84E-03	2.33E-03	2.04E-03	2.59E-03
Total environmental impacts	points	1.11E-02	9.50E-04	8.09E-03	1.42E-02	1.11E-02	9.41E-03	1.25E-02

Table S3. Results of Monte Carlo simulation for assessing the environmental impact of TiO_2 @Ti-F

Impact categories	Units	Mean TEI	Standard deviation	Minimum TEI	Maximum TEI	Median TEI	5% Percentile	95% Percentile
ecosystem quality - agricultural land occupation	points	1.46E-06	1.43E-07	1.00E-06	1.93E-06	1.47E-06	1.22E-06	1.67E-06

ecosystem quality - climate change, ecosystems	points	1.12E-03	9.27E-05	8.25E-04	1.42E-03	1.12E-03	9.61E-04	1.27E-03
ecosystem quality - freshwater ecotoxicity	points	5.11E-07	4.43E-08	3.71E-07	6.55E-07	5.13E-07	4.31E-07	5.78E-07
ecosystem quality - freshwater eutrophication	points	1.23E-06	1.16E-07	8.67E-07	1.62E-06	1.24E-06	1.03E-06	1.41E-06
ecosystem quality - marine ecotoxicity	points	1.45E-04	1.39E-05	1.02E-04	1.91E-04	1.46E-04	1.21E-04	1.67E-04
ecosystem quality - natural land transformation	points	3.50E-04	3.31E-05	2.46E-04	4.58E-04	3.51E-04	2.92E-04	4.00E-04
ecosystem quality - terrestrial acidification	points	4.22E-06	3.51E-07	3.10E-06	5.36E-06	4.24E-06	3.61E-06	4.77E-06
ecosystem quality - terrestrial ecotoxicity	points	3.56E-06	3.09E-07	2.59E-06	4.57E-06	3.58E-06	3.01E-06	4.03E-06
ecosystem quality - total	points	1.54E-03	1.33E-04	1.12E-03	1.98E-03	1.55E-03	1.30E-03	1.74E-03
ecosystem quality - urban land occupation	points	1.16E-05	1.11E-06	8.10E-06	1.53E-05	1.16E-05	9.69E-06	1.33E-05
human health - climate change, human health	points	1.41E-03	1.17E-04	1.04E-03	1.79E-03	1.42E-03	1.21E-03	1.59E-03
human health - human toxicity	points	4.13E-03	3.94E-04	2.88E-03	5.41E-03	4.14E-03	3.43E-03	4.72E-03
human health - ionising radiation	points	6.62E-07	6.43E-08	4.57E-07	8.76E-07	6.63E-07	5.48E-07	7.57E-07
human health - ozone depletion	points	1.05E-07	1.01E-08	7.29E-08	1.38E-07	1.05E-07	8.76E-08	1.20E-07
human health - particulate matter formation	points	2.50E-04	2.22E-05	1.81E-04	3.22E-04	2.51E-04	2.11E-04	2.84E-04
human health - photochemical oxidant formation	points	2.01E-05	1.42E-06	1.53E-05	2.44E-05	2.01E-05	1.78E-05	2.24E-05
human health - total	points	5.81E-03	5.33E-04	4.14E-03	7.56E-03	5.82E-03	4.87E-03	6.60E-03
resources - fossil depletion	points	1.87E-03	1.34E-04	1.44E-03	2.28E-03	1.88E-03	1.65E-03	2.08E-03
resources - metal depletion	points	1.05E-04	1.01E-05	7.28E-05	1.38E-04	1.05E-04	8.67E-05	1.20E-04
resources - total	points	1.93E-03	1.39E-04	1.48E-03	2.36E-03	1.93E-03	1.69E-03	2.15E-03
Total environmental impacts	points	9.44E-03	8.08E-04	6.88E-03	1.21E-02	9.44E-03	8.00E-03	1.06E-02

Table S4. Results of Monte Carlo simulation for assessing the environmental impact of 3DM-PbO_2/Ti

Impact categories	Units	Mean TEI	Standard deviation	Minimum TEI	Maximum TEI	Median TEI	5% Percentile	95% Percentile
ecosystem quality - agricultural land occupation	points	1.72E-06	1.68E-07	1.18E-06	2.27E-06	1.73E-06	1.43E-06	1.97E-06
ecosystem quality - climate change, ecosystems	points	1.32E-03	1.09E-04	9.70E-04	1.67E-03	1.32E-03	1.13E-03	1.49E-03
ecosystem quality - freshwater ecotoxicity	points	6.01E-07	5.21E-08	4.37E-07	7.71E-07	6.04E-07	5.07E-07	6.80E-07

ecosystem quality - freshwater eutrophication	points	1.45E-06	1.37E-07	1.02E-06	1.90E-06	1.46E-06	1.21E-06	1.66E-06
ecosystem quality - marine ecotoxicity	points	1.71E-04	1.63E-05	1.20E-04	2.25E-04	1.72E-04	1.42E-04	1.96E-04
ecosystem quality - natural land transformation	points	4.12E-04	3.89E-05	2.89E-04	5.39E-04	4.13E-04	3.43E-04	4.70E-04
ecosystem quality - terrestrial acidification	points	4.97E-06	4.13E-07	3.65E-06	6.31E-06	4.99E-06	4.25E-06	5.61E-06
ecosystem quality - terrestrial ecotoxicity	points	4.19E-06	3.63E-07	3.05E-06	5.38E-06	4.21E-06	3.54E-06	4.74E-06
ecosystem quality - total	points	1.93E-03	1.66E-04	1.40E-03	2.47E-03	1.94E-03	1.63E-03	2.18E-03
ecosystem quality - urban land occupation	points	1.37E-05	1.31E-06	9.53E-06	1.80E-05	1.37E-05	1.14E-05	1.57E-05
human health - climate change, human health	points	1.66E-03	1.38E-04	1.22E-03	2.10E-03	1.67E-03	1.42E-03	1.87E-03
human health - human toxicity	points	4.86E-03	4.64E-04	3.39E-03	6.37E-03	4.87E-03	4.03E-03	5.55E-03
human health - ionising radiation	points	7.79E-07	7.56E-08	5.38E-07	1.03E-06	7.80E-07	6.45E-07	8.90E-07
human health - ozone depletion	points	1.24E-07	1.19E-08	8.58E-08	1.62E-07	1.24E-07	1.03E-07	1.41E-07
human health - particulate matter formation	points	2.94E-04	2.61E-05	2.13E-04	3.79E-04	2.95E-04	2.48E-04	3.34E-04
human health - photochemical oxidant formation	points	2.37E-05	1.67E-06	1.80E-05	2.87E-05	2.37E-05	2.09E-05	2.64E-05
human health - total	points	6.83E-03	6.27E-04	4.87E-03	8.89E-03	6.85E-03	5.73E-03	7.77E-03
resources - fossil depletion	points	2.20E-03	1.58E-04	1.69E-03	2.68E-03	2.21E-03	1.94E-03	2.45E-03
resources - metal depletion	points	1.23E-04	1.19E-05	8.56E-05	1.62E-04	1.24E-04	1.02E-04	1.41E-04
resources - total	points	2.33E-03	1.68E-04	1.78E-03	2.84E-03	2.33E-03	2.04E-03	2.59E-03
Total environmental impacts	points	1.11E-02	9.50E-04	8.09E-03	1.42E-02	1.11E-02	9.41E-03	1.25E-02

Table S5. Results of Monte Carlo simulation for assessing the environmental impact of BDD/Ti

Impact categories	Units	Mean TEI	Standard deviation	Minimum TEI	Maximum TEI	Median TEI	5% Percentile	95% Percentile
ecosystem quality - agricultural land occupation	points	1.72E-06	1.68E-07	1.18E-06	2.27E-06	1.73E-06	1.43E-06	1.97E-06
ecosystem quality - climate change, ecosystems	points	1.32E-03	1.09E-04	9.70E-04	1.67E-03	1.32E-03	1.13E-03	1.49E-03
ecosystem quality - freshwater ecotoxicity	points	6.01E-07	5.21E-08	4.37E-07	7.71E-07	6.04E-07	5.07E-07	6.80E-07
ecosystem quality - freshwater eutrophication	points	1.45E-06	1.37E-07	1.02E-06	1.90E-06	1.46E-06	1.21E-06	1.66E-06
ecosystem quality - marine ecotoxicity	points	1.71E-04	1.63E-05	1.20E-04	2.25E-04	1.72E-04	1.42E-04	1.96E-04
ecosystem quality - natural land transformation	points	4.12E-04	3.89E-05	2.89E-04	5.39E-04	4.13E-04	3.43E-04	4.70E-04
ecosystem quality - terrestrial acidification	points	4.97E-06	4.13E-07	3.65E-06	6.31E-06	4.99E-06	4.25E-06	5.61E-06

ecosystem quality - terrestrial ecotoxicity	points	4.19E-06	3.63E-07	3.05E-06	5.38E-06	4.21E-06	3.54E-06	4.74E-06
ecosystem quality - total	points	1.93E-03	1.66E-04	1.40E-03	2.47E-03	1.94E-03	1.63E-03	2.18E-03
ecosystem quality - urban land occupation	points	1.37E-05	1.31E-06	9.53E-06	1.80E-05	1.37E-05	1.14E-05	1.57E-05
human health - climate change, human health	points	1.66E-03	1.38E-04	1.22E-03	2.10E-03	1.67E-03	1.42E-03	1.87E-03
human health - human toxicity	points	4.86E-03	4.64E-04	3.39E-03	6.37E-03	4.87E-03	4.03E-03	5.55E-03
human health - ionising radiation	points	7.79E-07	7.56E-08	5.38E-07	1.03E-06	7.80E-07	6.45E-07	8.90E-07
human health - ozone depletion	points	1.24E-07	1.19E-08	8.58E-08	1.62E-07	1.24E-07	1.03E-07	1.41E-07
human health - particulate matter formation	points	2.94E-04	2.61E-05	2.13E-04	3.79E-04	2.95E-04	2.48E-04	3.34E-04
human health - photochemical oxidant formation	points	2.37E-05	1.67E-06	1.80E-05	2.87E-05	2.37E-05	2.09E-05	2.64E-05
human health - total	points	6.83E-03	6.27E-04	4.87E-03	8.89E-03	6.85E-03	5.73E-03	7.77E-03
resources - fossil depletion	points	2.20E-03	1.58E-04	1.69E-03	2.68E-03	2.21E-03	1.94E-03	2.45E-03
resources - metal depletion	points	1.23E-04	1.19E-05	8.56E-05	1.62E-04	1.24E-04	1.02E-04	1.41E-04
resources - total	points	2.33E-03	1.68E-04	1.78E-03	2.84E-03	2.33E-03	2.04E-03	2.59E-03
Total environmental impacts	points	1.11E-02	9.50E-04	8.09E-03	1.42E-02	1.11E-02	9.41E-03	1.25E-02

Table S6. Percentage contents of Ti and O in Ti-F and TiO_2-OV@Ti-F anodes derived from SEM-EDS

Elements	Ti atom (%)	O atom (%)
Ti-F	97.00	3.00
TiO_2-OV@Ti-F	87.00	13.00

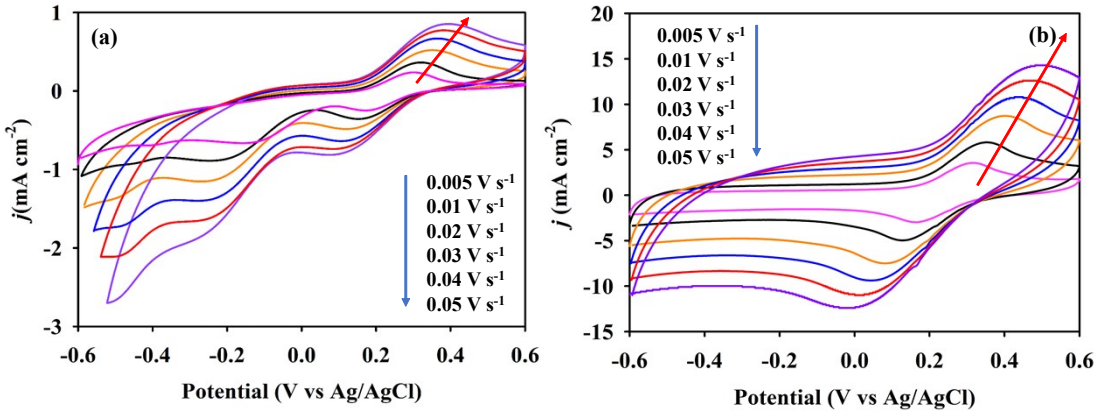

Fig. S4. Cyclic voltammograms of Ti-F, (a), and TiO_2-OV@Ti-F, (b), electrodes at different scan rates in supporting electrolyte containing 5 mM K3[Fe(CN)$_6$] and 0.1 M KCl at room temperature.

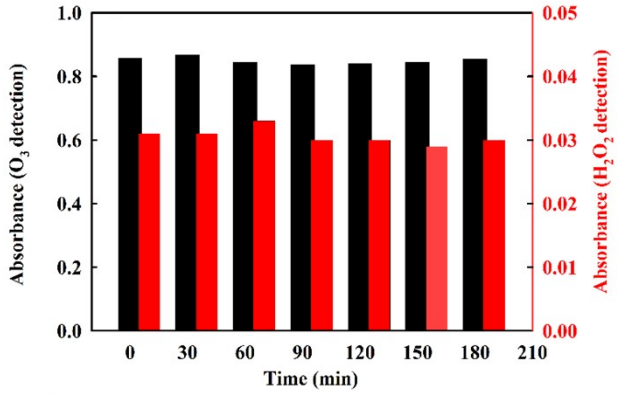

Fig. S5. Detection of O_3 and H_2O_2 on anode using Pt sheet cathode and TiO_2-OV@Ti-F anode at [Na_2SO_4] = 50 mM and current density=25 mA cm^{-2}.

Fig. S6. Gas bubble on the static TiO_2-OV@Ti-F anode observed by camera (AFT-ZL0920). Conditions: $[Na_2SO_4]$ = 50 mM and current density=25 mA cm^{-2}.

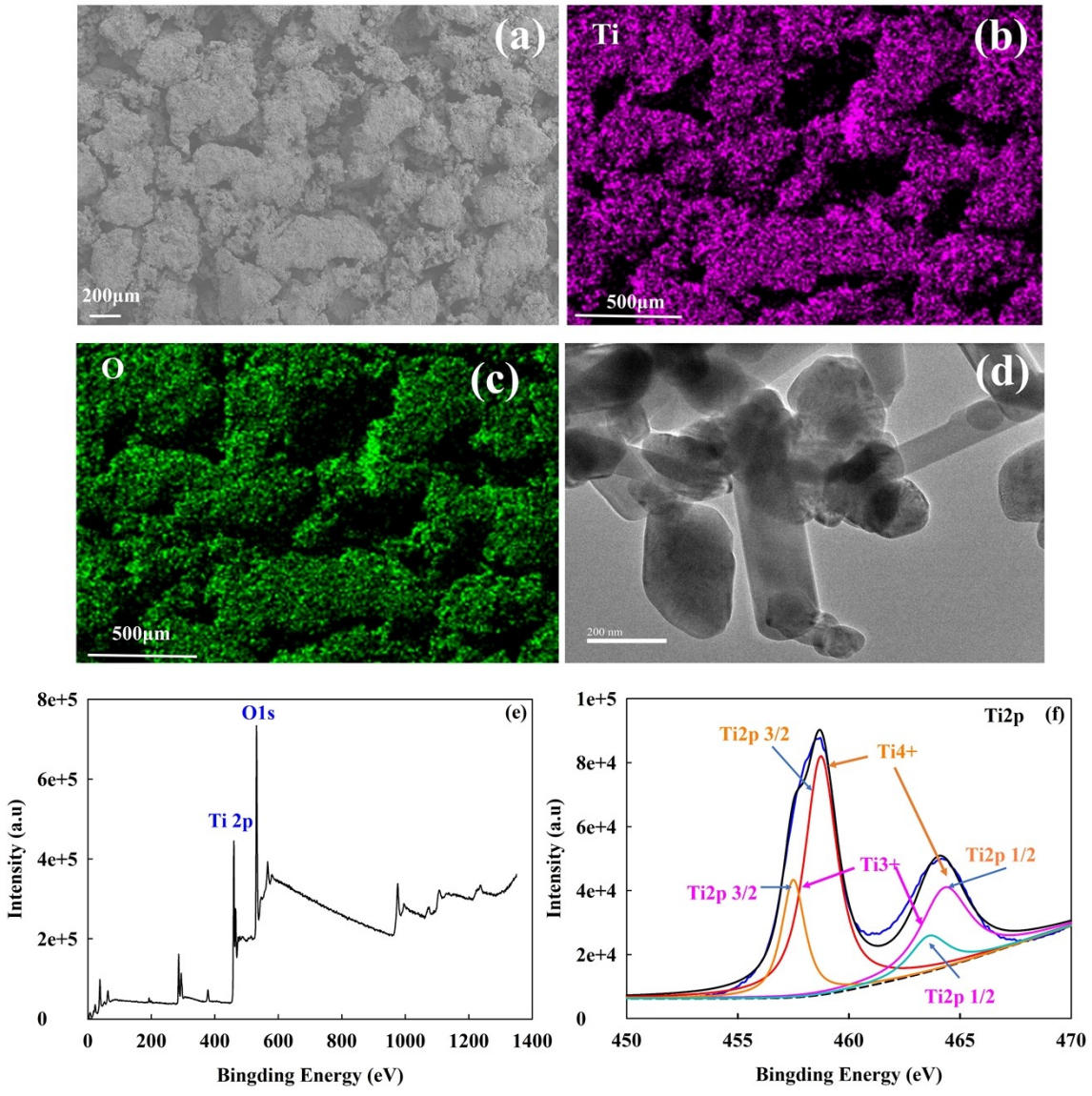

Fig. S7. (a-c) SEM images and (d) HRTEM, (c) whole spectrum (d) Ti2p of the regenerated TiO_2-OV@Ti-F anode

After fitting the Ti2p spectrum (Fig. S6c-d), we could deduce that the binding energy peaks at 464.07 and 458.78 eV are corresponded to 2p1/2 and 2p3/2 of Ti^{4+}, while binding energy at 463.73 eV and 457.49 eV are related to 2p1/2 and 2p3/2 of Ti^{3+} [7]. Based on the fitting area, the concentration of Ti^{3+} was approximately 26.32%.